

## Preparation and Characterization of CeO<sub>2</sub>doped ZnO-TiO<sub>2</sub>Semiconducting Nano Composite

H. Srinivasa Varaprasad<sup>1</sup>, Prof. P. V. Sridevi<sup>2</sup>, Dr. M. Satya Anuradha<sup>3</sup>

<sup>1</sup>(Research Scholar, Center for Nanotechnology,AUCE(A), Visakhapatnam, Andhra Pradesh, India)

<sup>2</sup>(Professor, Department of ECE, AUCE(A), Visakhapatnam, Andhra Pradesh, India)

<sup>3</sup>(AssociateProfessor, Department of ECE, AUCE(A), Visakhapatnam, Andhra Pradesh, India)

Corresponding Author : H. Srinivasa Varaprasad

---

**Abstract :** In this paper a new approach entitled MechanoGelation was introduced for the synthesis of CeO<sub>2</sub> doped ZnO-TiO<sub>2</sub> nanocomposite (CZT). Commercial ZnO and TiO<sub>2</sub>Nanopowders are mixed at the weighted percentage of 1:1and added with different molarities (0.1M and 0.2M) of CeO<sub>2</sub>Nanopowder. Further it was processed in a wet ball milling method in isopropanol solution followed by gelation. The prepared samples are calcinated at 450°C using the furnace.The powder X-Ray Diffraction analysis confirms that the diffraction peaks and phases of ZnO, TiO<sub>2</sub>and the existence of CeO<sub>2</sub> dopant in Nanocomposite. The Absorbance and Transmittance properties studied by UV-Visible spectroscopy, illustrate thatthe optical properties and Bandgap of the nanocomposite.The Transmission spectra is plotted by using Beer' s Law.Particle size, chemical composition, and surface morphology were studied using FESEM-EDS.

**Keywords:** Beer's Law, CeO<sub>2</sub>,Mechano Gelation,Ternary Nanocomposite,TiO<sub>2</sub>-ZnO.

---

Date of Submission: 25-08-2018

Date of acceptance: 08-09-2018

---

### I. INTRODUCTION

In recent years, considerable attention has been given to the study of the Ternary Metal Oxides based on ZnO and TiO<sub>2</sub> with metal oxide dopants like SnO<sub>2</sub>, CeO<sub>2</sub>, CuO, Fe<sub>2</sub>O<sub>3</sub>etc.due to their exceptional optical, electrical, dielectric and sensing properties in adoptable field of applications such as photocatalysis, solar cells, sensors, water purifiers, UV radiant protectors and batteries etc. [1-7].

Titanium dioxide is a semiconductor metal oxide and has unique properties like stable towards corrosion, photo-corrosion, inert, transparent and inexpensive. But electron-hole (e<sup>-</sup> - h<sup>+</sup>) recombination process decreases the efficiency of TiO<sub>2</sub> during oxidation-reduction. One of the approaches to overcome this problem has been the use of coupled semiconductor metal oxides that can reduce the recombination rate and increase its efficiencyasa catalyst [8].

ZnO is another important n-type semiconductor. Many superior physical properties, such as high electron mobility (~100 cm<sup>2</sup>V<sup>-1</sup>s<sup>-1</sup>), high thermal conductivity, large exciton binding energy(60meV), wide bandgap(3.36 eV) make it an active material for a wide range of applications, such as photocatalyst, sensor, pigment in paint, and can be implemented into semiconductor devices such as thin film transistors and thin film photovoltaic devices etc [9].

BesidesZnO and TiO<sub>2</sub> have similar band gaps, the coupling of different semiconductors has been proposed for the design of sensor systems to improve the oxidation-reduction of individual semiconductors.An appropriate combination of the conduction bands (CB) and the valence bands (VB) edges of both semiconductors can generate a transfer vector of photogenerated charge carriers from one to another, which can decrease their recombination. This can improve sensing properties.

ZnTiO<sub>3</sub>is a multi-functional material has been received considerable attention in various fields like photocatalysis, di-electric material, paint pigments, gas sensors, photoluminescence material etc. [10-13] CeO<sub>2</sub> is one of the favorable materials doped to ZnO and TiO<sub>2</sub> which affects morphological, electrical properties and improve absorption capacity [14-17].

The preparation of ZnO-TiO<sub>2</sub>-CeO<sub>2</sub> is done with hydrothermal, sol-gel, precipitation-decomposition, combustion and mechanical methods [18-20].

### II. EXPERIMENTAL

#### 2.1 Reagents and Chemicals:

ZnONanopowder (99.9% pure), TiO<sub>2</sub> Nano Powder(Anatase 99.9%pure), CeO<sub>2</sub> (99.9% pure), isopropanol, NaOH, deionized water, ethanol, Acetone.

## 2.2 Preparation for Nano-Composite:

A novel method was used to synthesize CeO<sub>2</sub> doped ZnO-TiO<sub>2</sub> nanocomposite. Commercial Nanopowders with 99.9% pure ZnO-TiO<sub>2</sub> mixed at 1:1 weighted ratio then 0.1M and 0.2M CeO<sub>2</sub>Nanopowder added to the composite. The prepared powder is ball milled at 600r.p.m for 45 min in a 125ml jar with 1:10 zirconium balls and isopropanol as a medium in high energy ball mill. These samples are collected and magnetically stirred for 6 hours at 550 r.p.m at room Temperature, 50ml deionized water and 20 mMol of NaOH is added. Further samples are stirred at 60°C for 3hrs with 250 rpm and gel samples were collected for fabrication. Collected gel samples are heated up to 85°C for 1hr on a heating mount. Samples were calcinated up to 450°C for 2hrs with an increment of 5°C/min in muffle furnace. 0.1M and 0.2M CeO<sub>2</sub>-ZnO-TiO<sub>2</sub> composite are named as C1A0, C2A0 and calcinated Samples are named as C1A450, C2A450.

## 2.3 Characterization:

The Crystalline size and phase structures of the samples were determined by XRD patterns which were obtained on Pan Analytical, X-Pert pro, X-ray diffractometer using CuK $\alpha$  radiation with  $\lambda=1.54060\text{nm}$  and the optical properties were calculated by plot analysis of electronic spectra obtained from Shimadju, UV-VIS Spectrophotometer. The surface morphology, particle size, the elemental analysis determined by JEOL Asia PTE Ltd, FESEM-EDS.

## III. RESULTS AND DISCUSSION

### 3.1 XRD:

Diffraction peaks in Figure1 describe ZnO, TiO<sub>2</sub>, CeO<sub>2</sub> peaks matched with JCPDS data, TiO<sub>2</sub> is in anatase phase and CeO<sub>2</sub> sufficiently doped to composite, no other peaks existed means fewer impurities in MachanoGelation process. The peaks of ZnTiO<sub>3</sub> shows equal strength of ZnO and TiO<sub>2</sub>. Table 1 represents Bragg angles with miller values, unit cell parameters with its Crystal Structure.

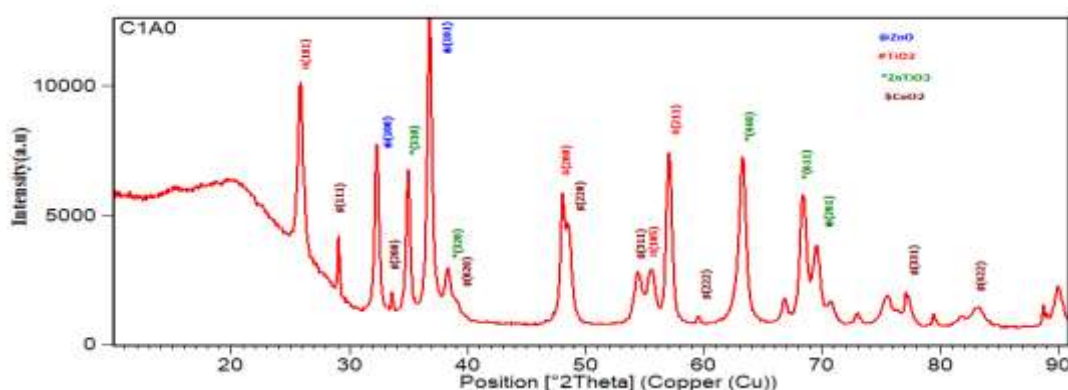


Figure 1 : XRD PEAKS of ZnO, TiO<sub>2</sub>, CeO<sub>2</sub>, ZnTiO<sub>3</sub>.

Bragg angle= $10^\circ \leq 2\theta \leq 90^\circ$   
Anode Cu, K  $\alpha=1.5406\text{\AA}$   
scanning rate=  $2^\circ/\text{min}$

Table I : XRD DATA of ZnO, TiO<sub>2</sub>, CeO<sub>2</sub>, ZnTiO<sub>3</sub>

S.No	MATERIAL	2 $\theta$	(h k l)	UNIT CELL	CRYSTAL STRUCTURE	#JCPDS
1	ZnO	32°, 36°	(100), (101)	a=3.2342 Å, c=5.1772 Å	Hexagonal	#89-0510
2	TiO <sub>2</sub>	25°, 38°, 56°, 58°	(101), (200), (105), (211)	a=3.7300 Å, c=9.3700 Å	Tetragonal	#21-1272
3	CeO <sub>2</sub>	28°, 34°, 39°, 54°, 59°, 78°	(110), (200), (020), (222), (331)	a=5.3623 Å, b=5.3263 Å, c=5.3623 Å	Triclinic (anorthic)	#81-0792
4	ZnTiO <sub>3</sub>	35°, 39°, 63°, 68°	(310), (320), (440), (611)	a=5.0748 Å, c=13.9267 Å	Cubic and hexagonal	#26-1500

The phase identification of prepared samples was carried out by XRD showed a single-phase nature of ZnO-TiO<sub>2</sub>. The patterns for the composite revealed the presence of reflections from both ZnO and TiO<sub>2</sub>with the equal Crystalline distribution of the phases within the sample.

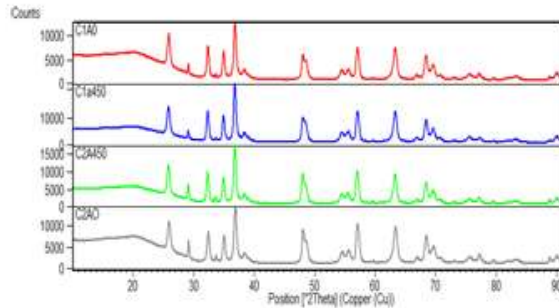


Figure 2: XRD PEAKS of C1A0, C1A450, C2A450, C2A0

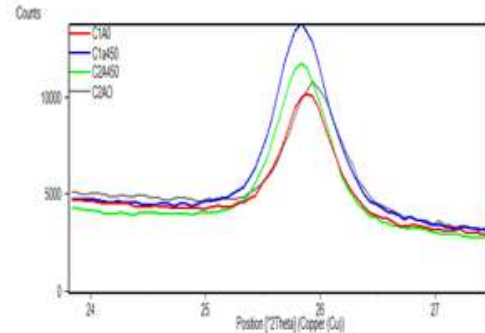


Figure 3: TiO<sub>2</sub>PEAK at (101)

Figure 2 represents different samples of CeO<sub>2</sub>at different molarities (0.1M,0.2M) doped with ZnO:TiO<sub>2</sub> composite at two different temperature (85°C,450°C). Figure 3 represents the phase of sample TiO<sub>2</sub> at (101).The phases after calcination is almost same and the crystalline size become more uniform.

Particle sizes were estimated from Scherrer relation which depends on the diffraction angle  $\theta$ .

$$D = \frac{K\lambda}{\beta \cos \theta}$$

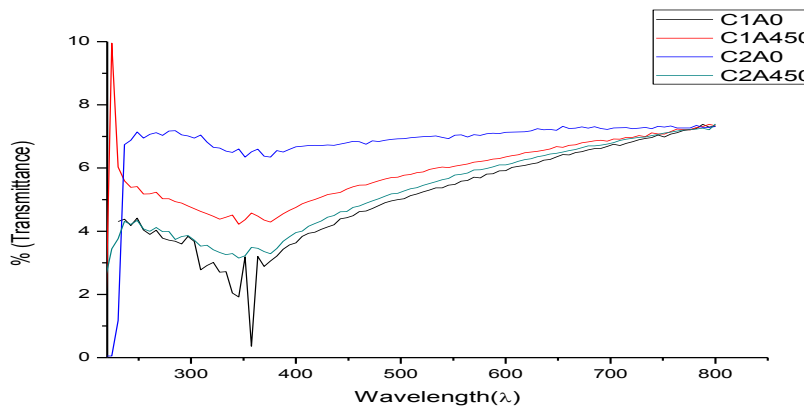
Where D is grain size,  $\lambda$  is the wavelength of the used X-ray radiation, K is the constant equal to 0.9,  $\beta$ hkl is the full width at half maximum (FWHM) of the diffraction peak and  $\theta$  is its Bragg diffraction angle. Particle sizes are registered as 4.34nm, 5.68nm, 5.44nm, 5.50nm as listed in table 2.

Table II : Crystalline size at 0.1M and 0.2M at Temperature 85 °C and 450 °C

S.NO	CeO <sub>2</sub> %	TEMP(°C)	CRYSTALLINESIZE(nm) FROM XRD	PARTICLE SIZE FROM FESEM(nm)
1	0.1M	85 °C	4.34	55.4
2	0.2M	85 °C	5.44	37.6
3	0.1M	450 °C	5.68	40.2
4	0.2M	450 °C	5.50	37.5

### 3.2 Optical Properties from UV-VISSpectroscopy:

The optical transmittance, absorbance, and the band gap values (E<sub>g</sub>) of CZT Nanopowders as a function of molarities 0.1M and 0.2M at 85°C and at 450°C has been studied. Figure 4 shows the optical transmittance of the composite.It was measured in the range of wavelength 200 to 800 nm. The transmittance spectra revealed that low average transmittance between 1% – 7.5% within the visible region (250 - 800 nm). The transmission decreases sharply to about 360 nm of the composite due to the band gap absorption.



**Figure 4: UV Transmittance Spectra**

Bandwidth are calculated using the equation

$$E_g = \frac{1240}{\lambda}$$

Bandwidth is calculated as listed in Table3. The transmittance spectra plotted from absorbance spectra using Beer's Law

$$A = 2 - \log_{10} (\%T)$$

Absorbance Decreases with increase in dopant of CeO<sub>2</sub> because of Crystal size. But increases after calcination.

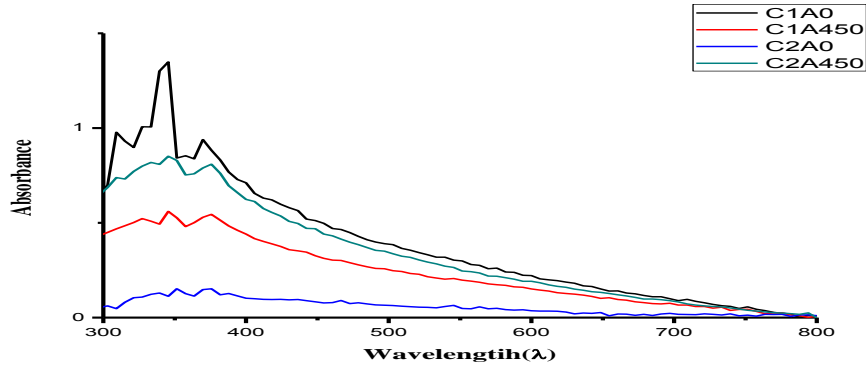


**Figure 5: UV- Absorbance Spectra**

**Table III : OpticalBandgaps of samples**

Material	Maximum absorbance at the wavelength	Bandgap
C1A0	397.43	3.12
C2A0	381.53	3.25
C1A450	359.42	3.45
C2A450	347.33	3.57

Figure 5 represents absorbance spectra of CZT nanocomposite, maximum absorbance is identified at 347nm to 398 nm. Which is in visible region. The composite material remains better visible light transmission and visible light absorbance material.

Optical Bandwidth is in the range of 3.1 to 3.6. It is wide bandgap where wide bandgap materials are suitable for high temperature, high frequency, high power, high radiation applications

### 3.3 FESEM:

FESEM: Field Emission Scanning Electron Microscope was carried out to investigate morphology, size, and structure of metal oxide nanocomposites. Figure 6 shows the morphology of 0.1M and 0.2M CeO<sub>2</sub> doped to 1:1 ratio of ZnO and TiO<sub>2</sub> calcinated at 85°C and 450°C. Particle sizes were tabulated in the Table2. The grains are nearly spherical in shape and more porous with less diameter. The average diameter is in between 30nm to 60nm. The gap between spheres also very less. The grain sizes become less and more uniform after calcination.

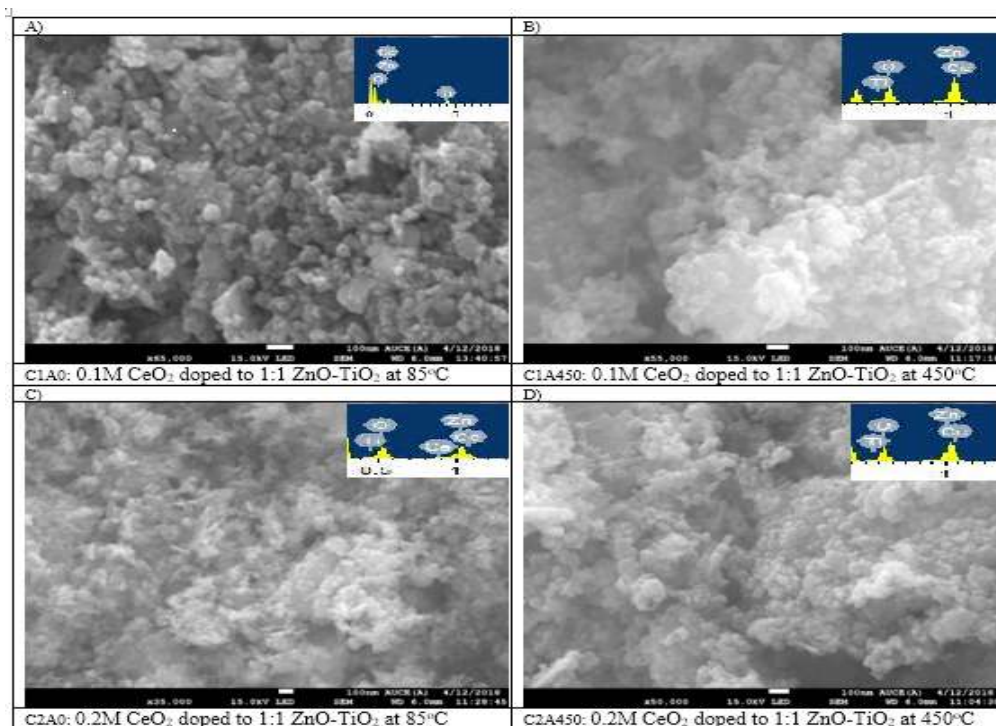


Figure 6: FE-SEM images of Nano Composite calcinated at 85°C and 450°C with 0.1 and 0.2M CeO<sub>2</sub>

Energy dispersive analysis of X-ray (EDAX) indicates that the composite contains only Zn, Ti, Ce, O elements, revealing the purity of the composite. From Table 4, it is observed that the percentage ratios of Zn, Ti was almost 1:1 ratio and amount of Ce dopant also existed in the ternary composite. The atomic percentage of Zn, Ti, Ce increases because of oxygen reduces after calcination.

Table IV: FESEM-EDAX analysis

S.no	Sample name	Atomic Percentages			
		Zn	Ti	Ce	O
1	C1A0	11.21	12.72	0.19	75.8
2	C2A0	11.39	12.33	0.36	75.9
3	C1A450	16.34	14.73	0.21	68.7
4	C2A450	13.92	15.63	0.46	69.9

#### IV. Conclusion:

(i) x-ray diffraction analysis confirms that ZnO and TiO<sub>2</sub> are successfully doped with CeO<sub>2</sub> and no other impurities are present in the prepared ternary composite. ZnO influences TiO<sub>2</sub> to maintain anatase phase even at higher temperature. ZnTiO<sub>3</sub> has mixed phase which is used in paints and pigment industries, photo catalysis and gas sensors. the average crystalline size is calculated to be 4-6 nm.

(ii) From UV-VIS Spectrophotometer analysis, Maximum absorbance is in visible region i.e 350 nm to 400 nm. TiO<sub>2</sub> anatase absorbs UV light with wavelengths close to the visible spectrum. This activates the titanium dioxide by exciting electrons to higher levels. Optical band gap is to be calculated 3.12eV to 3.57eV. bandgaps are increases with CeO<sub>2</sub> molarity and calcination temperature.

(iii) It is observed that from FESEM-EDS, the Average particle size is 50 to 60 nm and Particles are highly porous and uniformly distributed. The distance between particle to particle is also less.

(iv) High porosity and less diameter Nano powder composites are suitable for gas sensing applications. CeO<sub>2</sub> enhances the oxidation-reduction efficiency of the composite because of the oxygen absorption property. Both the absorbance and transmittance Wavelengths are in visible region so that optical and sensing applications can be done in the visible region.



**REFERENCES**

- [1]. Yang Shaogui, Quan Xie, Li Xinyong, Liu Yazi, "Preparation, characterization and photocatalytic properties of nanocrystalline Fe<sub>2</sub>O<sub>3</sub>/TiO<sub>2</sub>, ZnO/TiO<sub>2</sub>, and Fe<sub>2</sub>O<sub>3</sub>/ZnO/TiO<sub>2</sub> composite film electrodes towards pentachlorophenol degradation", *Chem. Chem. Phys.*, 6, 2004, p.659-664.
- [2]. R.B. Pedhekar, F.C. Raghuvanshi, V.D.Kapse, "Liquid petroleum gas sensing performance enhanced by CuO modification of nanocrystalline ZnO-TiO<sub>2</sub>", *Material Science-poland*, 34(3), 2016, p.571-581
- [3]. SarraAyed, Raoudha Ben Belgacem, Jaafar Othman Zayani, Adel Matoussi, "Structural and optical properties of ZnO/TiO<sub>2</sub> composites", *Superlattices and Microstructures*, 91, 2016, p.118-128.
- [4]. V. Rajendra, Y. raghu, B. rajithac, C.S.Chakrab, k.v. rao, s. H. park, "Synthesis, Characterization, and Photocatalytic behavior of nanocrystalline ZnO, TiO<sub>2</sub>, and ZnO/TiO<sub>2</sub> nanocomposites", *Journal of Ovonic Research*, 13(3), 2017, p. 101 – 111.
- [5]. C.M.Firdaus, M.S.B.ShahRizam, M.Rusop, S.RahmatulHidayah, "Characterization of ZnO and ZnO: TiO<sub>2</sub> Thin Films Prepared by Sol-Gel Spray-Spin Coating Technique", *Procedia Engineering* 41, 2012, P. 1367 – 1373.
- [6]. Pankaj Kumar Bait and J Manam, "Luminescence properties of ZnO/TiO<sub>2</sub> nanocomposite activated by Eu<sup>3+</sup> and their spectroscopic analysis", *Bull. Mater. Sci.*, 39(5), 2016, p 1233–1243.
- [7]. David Ramírez-Ortega, Angel M. Meléndez, Próspero Acevedo-Pena, Ignacio Gonzalez, Ruben Arroyo, "Semiconducting properties of ZnO/TiO<sub>2</sub> composites by electrochemical measurements and their relationship with photocatalytic activity", *Electrochimica Acta* 140(2014) 541-549.
- [8]. Guidong Yang, Zifengyan, Tiancumxiao, "Preparation and Characterization of SnO<sub>2</sub>/ZnO/TiO<sub>2</sub> Composite semiconductor with enhanced photocatalytic activity", *Applied Surface Science* 258, 2012, p.8704-8712.
- [9]. Zhong Lin Wan, "Zinc oxide nanostructures: growth, properties, and applications", *J. Phys. Condens. Matter* 16, 2004, p.829–858.
- [10]. Chakkaphanwattanawikkam, WisanuPecharapa "Optical, Dielectric and Photocatalytic Properties of Perovskite ZnTiO<sub>3</sub> Nanoparticle Synthesized by Sonochemical process", *IEEE*, 2015
- [11]. Xin Yan, Cui-lisan Zahao, Yi-long Zhao, Yi-long Zhou, "Synthesis and Characterization of ZnTiO<sub>3</sub> with high photocatalytic activity", *Nonferrous Met. Soc. China* 25, 2015, p.2272-228.
- [12]. Yee-Shin Chang, Yen-Hwei Chang, In-Gann Chen, "Synthesis, formation and characterization of ZnTiO<sub>3</sub> ceramics", *Ceramics International* 30, 2004, p.2183-2189.
- [13]. P. K. Jain, D. Kumar, A. Kumar, D. Kaur "Structural, optical and dielectric properties of ZnTiO<sub>3</sub> ceramics", *OptoElectronics and Advanced Materials – Rapid Communications*, 4(3), 2010, p. 299 – 304
- [14]. Oman Zuas, Nuryatini Hamim, "Synthesis, Characterization and Properties of CeO<sub>2</sub>-doped TiO<sub>2</sub> Composite Nanocrystals", *Materials science (MEDZIAGOTYRA)*. 19(4), 2013, p.443-447.
- [15]. Shichun Di, Yupeng Guo, Hongwei Lv, Jie Yu, Zhenwei Li, "Microstructure and properties of rare earth CeO<sub>2</sub>-doped TiO<sub>2</sub> nanostructured composite coatings via micro-arc oxidation", *Ceramics International* (2014).
- [16]. H. Colak, "Synthesis and characterization of CeO<sub>2</sub>-doped ZnO", *Kovove Mater.* 54, 2016, p. 107– 112.
- [17]. Katya Milenova I, Katerina Zaharieva, Irina tambolova, Vladimir Blaskov, Alexander Eliyas, Ljubomir Dimitrov, "Photocatalytic performance of TiO<sub>2</sub>, CeO<sub>2</sub>, ZnO and TiO<sub>2</sub>-CeO<sub>2</sub>-ZnO in the course of methyl orange dye degradation", *Journal of Chemical Technology and Metallurgy*, 52(1), 2017, p.13 – 19.
- [18]. Xiuping li, Rongxiang Zhao, Vuchun Zhai and Peihua ma, "UV-Shielding and Photocatalytic Properties of ZnO-CeO<sub>2</sub>-TiO<sub>2</sub> Composite", *Asian Journal of Chemistry*, 26(15), 2014, p. 4566-4570.
- [19]. Xiuping li, Rong Xiang zhao, Heng Jiang, Vuchun Zhai and Peihua ma, "Preparation and Catalytic Properties of ZnO-CeO<sub>2</sub>-TiO<sub>2</sub> Composite", *Synthesis and Reactivity in Inorganic, Metal-Organic, and Nano-Metal Chemistry*, 46, 2016, p. 775–782.
- [20]. S.Prabhu, T.Viswanathan, K.Jothivenkatachalam, and K.Jeganathan "Visible light Photocatalytic activity of CeO<sub>2</sub>-ZnO-TiO<sub>2</sub> Composite for the degradation of Rhodamine B", *Indian Journal Of Material Science*, 2014, p.1-10

H. Srinivasa Varaprasad "Preparation and Characterization of CeO<sub>2</sub>doped ZnO-TiO<sub>2</sub>Semiconducting Nano Composite "International Journal of Engineering Science Invention(IJESI), vol. 7, no. 8, 2018, pp. 28-33